Оптический журнал

Лазерная физика и техника

Two-dimensional environment reconstruction based on absolute local deflection angle of laser scanning data

© 2019 Chunyong Wang, Jiancheng Lai, Bo Tang, Wei Yan, Yunjing Ji, Zhenhua Li

Department of Information Physics and Engineering, Nanjing University of Science and Technology, Nanjing, China

E-mail: laijiancheng@njust.edu.cn

Submitted 04.07.2018

DOI:10.17586/1023-5086-2019-86-02-29-35

Successive edge following (SEF) is extensively used to extract environment characteristics from two-dimensional laser scanning data given its simplicity. Conventional SEF compares the Euclidean distance between two adjacent points to either a fixed or an adaptive threshold. However, the segmentation accuracy is low and information loss occurs during processing of planes with large deflection angle with respect to the laser sensor, because the distance estimation is sensitive to this angle. Moreover, available SEF algorithms cannot suitably determine corners in the environment. To address these problems, we propose an extended SEF algorithm based on the absolute local deflection angle of laser scanning points. The proposed algorithm determines the local deflection angle between target and reference points, and an adaptive threshold is calculated based on the range precision of the laser sensor. Furthermore, corners are efficiently estimated and noise is mitigated by using three constraints. An experiment on two-dimensional environment reconstruction of an underground parking lot verifies the accuracy and capability of the proposed algorithm to reconstruct the lines and corners representing the environment.

Keywords: *successive edge following, laser sensor, laser scanning, feature extraction, corner detection.*

OCIS codes: *280.3420, 280.3400, 040.1880.*

Восстановление пространственного окружения при двумерном лазерном сканировании, использующее данные об абсолютной величине локального угла отклонения

© 2019 г. Chunyong Wang, Jiancheng Lai, Bo Tang, Wei Yan, Yunjing Ji, Zhenhua Li

Благодаря свое простоте, алгоритм последовательного отслеживания границы (Successive edge following (SEF)) широко применяется для извлечения характеристик окружения из данных двумерного лазерного сканирования. Обычно в методе SEF сравнивается эвклидово расстояние между двумя соседними точками с фиксированным или адаптивно изменяющимся пороговым значением. Однако точность сегментации оказывается небольшой, и происходит потеря информации при обработке плоскостей, отвечающих большим углам отклонения сканирующего излучения, поскольку оценка расстояния между точками чувствительна к этому углу. Помимо этого, обычные алгоритмы SEF не позволяют удовлетворительно распознавать наличие углов в окружении. Для преодоления этих недостатков предложен расширенный алгоритм SEF, использующий данные об абсолютном значении углов отклонения сканирующего лазерного излучения. В нём определяется локальный угол между объектом и референтными точками и вычисляется значение адаптивного порога на основе точностных параметров лазерного датчика. Показано, что с использованием указанного подхода успешно определяются углы, а также происходит подавление шума. Эксперимент по двумерному восстановлению обстановки в помещении подземного паркинга подтвердил соответствие полученной картины реальности и способность алгоритма к распознаванию линий и углов, представляющих окружение.

Ключевые слова: *последовательное отслеживание границы, лазерный датчик, лазерное сканирование, выделение признаков, распознавание углов.*

1. INTRODUCTION

Two-dimensional (2D) laser sensors offer fast, stable, and accurate distance measurements and have been widely used for environment perception in mobile robots [1, 2]. In fact, perception systems based on 2D scanning laser sensors can endow robots with localization, mapping, and path planning capabilities [3]. This information can be geometrically obtained in the plane by determining lines, corners, and arcs characterizing the environment surfaces from range data acquired by the laser sensor. In particular, lines suitably represent the complex but highly structured office environments. Therefore, the accurate and efficient extraction of line information is an essential process for automatic localization and navigation of mobile robots.

Over the last decades, several algorithms to extract lines from 2D range scans have been proposed, mainly comprising methods based on point distance [4, 5], Kalman filtering [6], image processing [7], and the Bayesian approach [8]. Methods based on point distance have been widely used and include successive edge following (SEF) [9], line tracking [10], iterative end-point fitting [11], split and merge [12], random sampling consensus [13], and Hough transform algorithms [14]. Among them, SEF has been extensively studied and applied given its simplicity, as it separates line segments when the distance among two adjacent points is larger than a threshold.

However, the conventional SEF algorithm uses a fixed threshold to segment the scanning points into different lines, thus reducing the segmentation accuracy when determining the structure of environments with target surfaces at different distances. Bu et al. [15] improved SEF by proposing an adaptive distance threshold computed from the polar radius-arc relation. The polar radius is the average distance among adjacent points around a reference point. However, the estimated distance between two points measured by a laser sensor is affected by the relative tilt angle when scanning the surface. Hence, the improved SEF algorithm removes points with large angles with respect to the laser sensor from the measured surfaces (e.g., wall sides and columns), thus leading to information loss. On the other hand, laser data are always corrupted by missing distance information and outliers caused by erroneous and noisy distance information. Consequently, conventional SEF is non-robust compared to recursive algorithms based on the Hough transform and random sampling consensus. In fact, conventional SEF algorithms cannot effectively remove noise. Moreover, the least squares method (LSM) that performs line fitting in SEF is highly sensitive to noise.

To solve the abovementioned problems, we propose an extended SEF algorithm based on the absolute local deflection angle instead of the distance among laser scanning points. The proposed algorithm considers both the distance to the target and the relative angle of the sensor to the measured surface. Consequently, it provides a more accurate clustering from more complete set points than similar SEF methods. Moreover, lines and corners can be estimated by directly applying the LSM, and the algorithm is robust to missing information and outliers, because it removes noisy points during segmentation.

The rest of this paper is organized as follows. In Sec. 2, the scanning model using a 2D laser sensor is introduced, and the shortcomings of existing SEF algorithms are analyzed. Section 3 details the proposed SEF algorithm with the corresponding segmentation and 2D reconstruction methods. In Sec. 4, the feature extraction and environment reconstruction capabilities of the proposed algorithm are applied and verified in an underground parking lot. Finally, we draw conclusions in Sec. 5.

2. BACKGROUND

2.1. Scanning model using 2D laser sensor

Laser detection and ranging or LADAR is an optical remote sensing technology for estimating the distance to targets by the emission and detection of laser pulses. By integrating a laser sensor with a rotating system, the distance from the system to surrounding surfaces can be obtained by sequential measurements as shown in Fig. 1, which illustrates a typical scanning process using a 2D laser sensor.

The points detected by the laser sensor are represented by $P = \{p_n(r_n, \theta_n) \,|\, n = 1, ..., N\}$, where (r_n, θ_n) are the polar coordinates of the n-th point, and the distance to the target surface, r_n, and angle θ_n between the point and a reference are given by

$$r_n = \frac{ct}{2}, \tag{1}$$

$$\theta_n = (n-1)\theta, \tag{2}$$

where c is the speed of light, t is the laser pulse time of flight, and θ is the angular resolution of the scan-

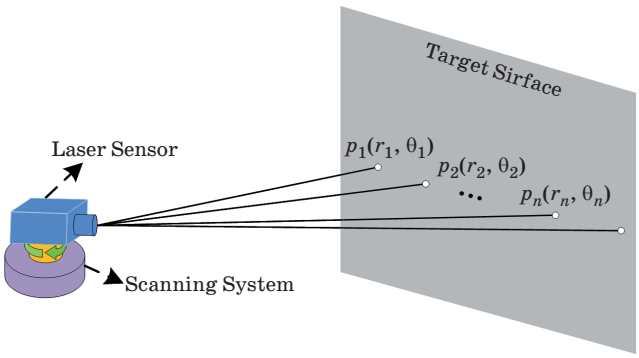

Fig. 1. Scanning process using 2D laser sensor.

ning system. Then, the Euclidean distance among two adjacent points, p_n and p_{n+1}, can be calculated by

$$D(p_n, p_{n+1}) = \sqrt{{r_n}^2 + {r_{n+1}}^2 - 2r_n r_{n+1}\cos\theta}. \quad (3)$$

2.2. SEF algorithms for segmentation

The conventional SEF algorithm segments the laser scanning data into point clusters by evaluating the Euclidean distance against a fixed threshold. However, this approach has a low performance when the environment presents considerable changes on the surface locations. To prevent this problem, the adaptive threshold SEF based on the polar radius-arc relation was proposed [15]. This improved SEF algorithm relies on an adaptive threshold to segment points. First, it calculates reference distance r'_n based on the adjacent points close to point p_n by

$$r'_n = \frac{\sum_{j=n-a}^{n+a} r_j}{a}, \quad (4)$$

where r_j is the distance of the j-th point to the target surface and a is the number of adjacent measurement points. The adaptive distance threshold is given by

$$DT_n = \alpha {r_n}', \quad (5)$$

where α is the scanning angular resolution. Therefore, this algorithm improves the segmentation accuracy for target surfaces at considerably different locations. However, it cannot deal with a situation such as that illustrated in Fig. 2, where the measured surface has a large deflection angle with respect to the laser sensor.

The relations among distances from points on the left, $D(p_{n-1}, p_n)$, and right, $D(p_{n-1}, p_n)$, of a reference point, and adaptive distance threshold DT_n

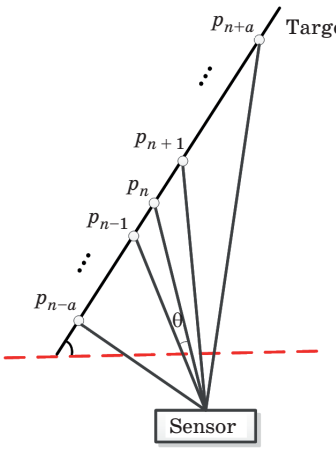

Fig. 2. Sensor surface measurements with large deflection angle.

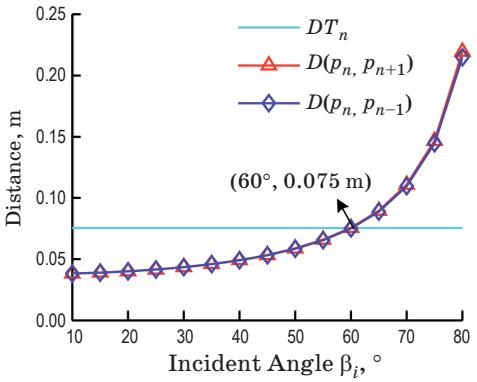

Fig. 3. Measured distance according to deflection angle using adaptive threshold SEF algorithm with $r_n = 20$ m, $\theta = 0.108°$ and $a = 3$.

calculated using Eqs. (4) and (5) according to the deflection angle are depicted in Fig. 3. The distance of the reference point is set as $r_n = 20$ m, the number of adjacent points on one side to $a = 3$, with scanning angular resolution of 0.108° corresponding to a sampling rate of 10×10^3 samples/s of the laser sensor and rotational speed of 3 rev/s of the scanning system. These are the parameters used for the experiment reported below.

Figure 3 shows that the distances of the points on the left and right of the reference are positively correlated to the increasing deflection angle to the target surface, and the relations are almost equal according to the angle. Moreover, for deflection angle above 60°, the distances in the figure are higher than the adaptive threshold, thus indicating that surface points measured at such angles are removed by the adaptive threshold SEF algorithm.

3. PROPOSED SEF ALGORITHM

3.1. Model

To improve segmentation accuracy, we propose an improved SEF algorithm based on local oscillation instead of distance. The geometric model of the scanning points using the local deflection angle of adjacent points is illustrated in Fig. 4.

Taking point p_n as reference, l_r is an auxiliary line perpendicular to the detecting optical path l_n of point p_n. In addition, we define angle φ_n^+ as the angle between points p_n and p_{n+1}. Hence, local deflection angle φ_n^+ satisfies

$$r_n \cos(i\theta) = r_{n+i} \cos\left(i\theta + {\varphi_n}^+\right). \quad (6)$$

Then, φ_n^+ can be calculated as

$$\varphi_n^+ = \operatorname{atan}\left(\frac{r_{n+i}\cos(i\theta) - r_n}{r_{n+i}\sin(i\theta)}\right). \quad (7)$$

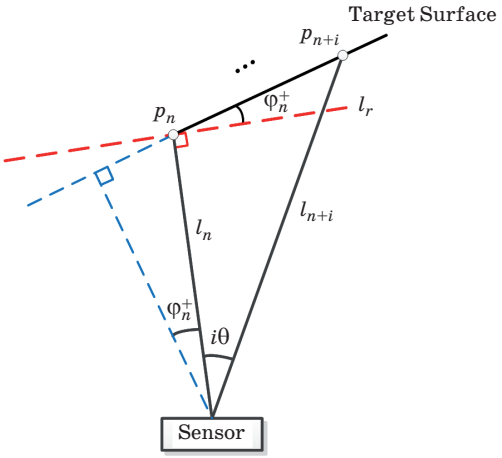

Fig. 4. Geometry of scanning points to define local oscillation angle.

Similarly, local deflection angle φ_n^- between points p_n and p_{n-i} is given by

$$\varphi_n^- = \operatorname{atan}\left(\frac{r_{n-i}\cos(i\theta) - r_n}{r_{n-i}\sin(i\theta)}\right). \quad (8)$$

Equations (7) and (8) demonstrate that the local deflection angles are nonnegative when $r_{n\pm i}\cos(i\theta) \geq r_n$. Therefore, the local deflection of reference point p_n is defined as

$$\varphi_n = \left|\varphi_n{}^+ + \varphi_n{}^-\right|, \quad (9)$$

with maximum value appearing on turning points, including columns and corners, as shown in Fig. 5.

Local oscillation φ_n of a flat target surface equals zero in the ideal case when the range precision of the laser sensor is zero. However, in practice, we should define a minimum detectable surface width in space L, because a laser scanning with fixed angular resolution retrieves a nonuniform point distribution for a given surface width at different distances. The angle between two measured points is equal to the angular resolution times i

$$i = \left\lfloor \frac{L}{\bar{r}_n \alpha} \right\rceil, \quad (10)$$

$$\bar{r}_n = \frac{\sum_{j=n-a}^{n+a} r_j}{2a+1}, \quad (11)$$

where r_n is the average distance of points close to p_n and the sign $'[\ ]'$ is the rounding function. Finally, we define the adaptive local deflection threshold, LDT_n, based on the precision of the laser sensor as

$$LDT_n = 2\operatorname{atan}\left|\cot(i\theta) - \frac{\bar{r}_n + \delta}{\bar{r}_n \tan(i\theta) - \delta\sin(i\theta)}\right|, \quad (12)$$

where δ is the range precision of the laser sensor.

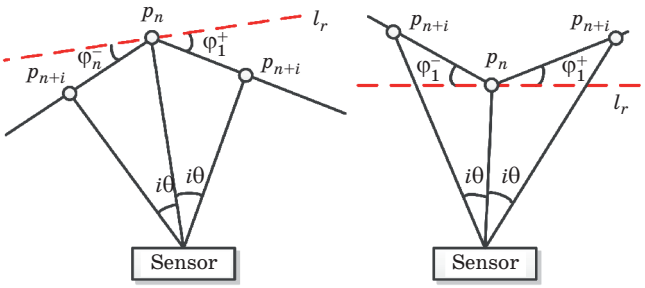

Fig. 5. Examples of maximum local oscillation with respect to reference point p_n.

3.2. Segmentation

The proposed SEF based on local oscillation allows to directly segment the laser scanning data into point clusters using the scanning points represented by (r_n, θ_n). Nevertheless, the data usually presents noise by outliers and missing information. We increase the robustness and efficiency of the proposed algorithm by including three constrains: (i) create a new segment when the distance to the target surface of the reference point is $r_n = 0$; (ii) segment the reference point from the front one, when the distance between two points satisfies $D(p_{n-1}, p_n) \geq D_T$, where D_T is a fixed threshold; (iii) remove the clusters with number of elements $m \leq M$, where M is the predefined minimum number of points per segment. Figure 6 shows the flowchart of the proposed SEF algorithm based on local deflection, which is described in the sequel.

The proposed algorithm first initializes the parameters, which we set for this study to minimum target width $L = 15$ m, scanning angle resolution $\theta = 0.108°$, range precision $\delta = 2$ cm, minimum number of points per segment $M = 3$, maximum distance threshold between adjacent points $D_T = 30$ cm, and number of adjacent points $a = 3$. Then, the algorithm evaluates constraints 1, 2, and 3, which are highlighted in Fig. 6. If the parameters computed by the current reference point do not satisfy any of the three constraints, the reference point is added to the current segment. Otherwise, the algorithm executes the segment processing stage, which is enclosed in the red rectangle in Fig. 6. Note that the third constraint comprises two steps to segment the optimal turning point with a maximum local oscillation. In the segment processing stage, a new segment is established if the number of points is higher than threshold M. Otherwise, the segment should include additional points. Finally, the next point is processed until considering all the reference points.

3.3. Line reconstruction

After segmentation, the point clusters are represented by sets $S_{i\ =\ 1,2,3...c} = \{p_{i1}(r_{i1}, \theta_{i1}), p_{i2}(r_{i2}, \theta_{i2}), ...,$

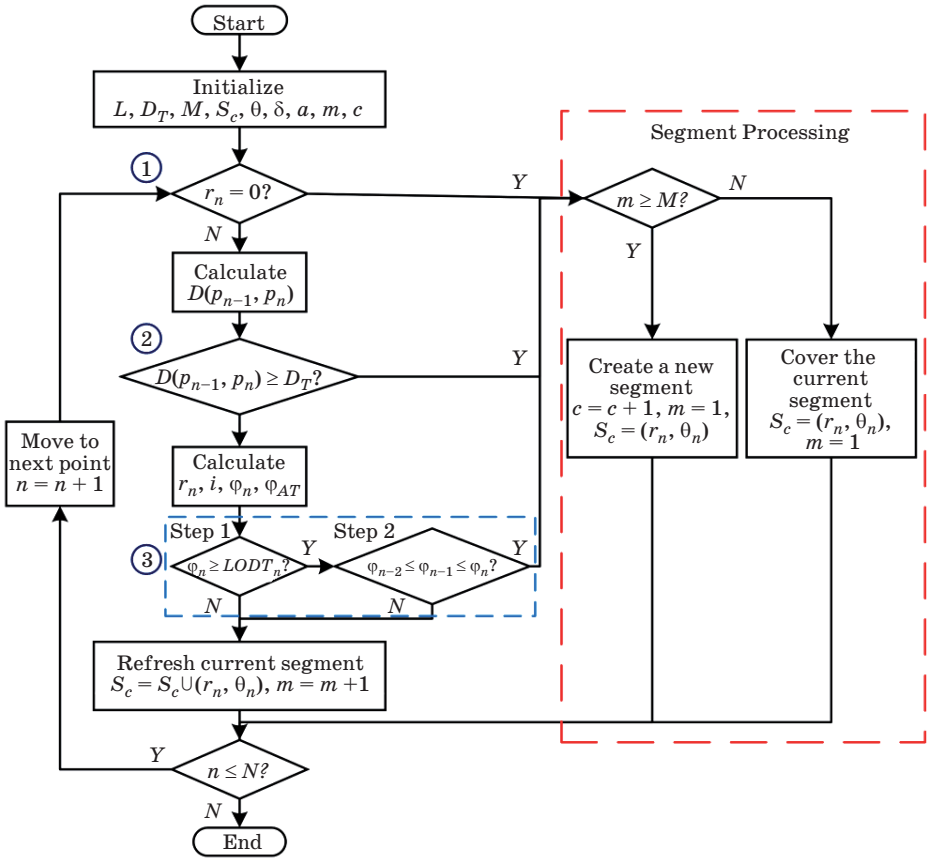

Fig. 6. Flowchart of proposed SEF algorithm based on local oscillation.

$p_{im}(r_{im}, \theta_{im}) \mid m \geq M\}$. The line parameters are estimated using the LSM in the form

$$y = kx + b, \tag{13}$$

where k and b are the slope and y-axis intercept of the line, respectively.

To avoid overfitting, we include a merge step to integrate two adjacent collinear sets S_i, S_{i+1} into one if the distance between the final point of S_i and the initial point of S_{i+1} is smaller than threshold D_T and the angle between two adjacent lines, computed using Eq. (14), is smaller than a threshold γ_T.

$$\gamma_{(S_i, S_{i+1})} = \arctan\left(\frac{k_{i+1} - k_i}{1 + k_{i+1}k_i}\right). \tag{14}$$

The merge step allows the efficient estimation of line segments. Then, after applying the LSM to determine all the segments, the corners can be determined from Eq. (14), thus generating the reconstructed environment plane.

4. EXPERIMENTAL RESULTS

We obtained the 2D environment reconstruction of an underground parking lot, thus verifying the complete and accurate estimation provided by the proposed algorithm. As mentioned above, the sampling rate of laser sensor is $10{\times}10^3$ samples/s and the maximum measuring distance is 50 m with a 2 cm range precision. In addition, the rotational speed of the scanning system is 3 rev/s, resulting in a 0.108° scanning angular resolution. The raw scanning points measured from the environment are shown in Fig. 7, where the red circle indicates the scanning system location. The environment measurements include three rectangular columns (red dashed rectangles), three embedded hollows (orange dashed ovals), three protruding structures (blue dashed ovals), outliers (black dashed circles), and scanned points corresponding to walls (unmarked blue solid line segments).

The segmentation results of the points obtained from different SEF algorithms are shown in Fig. 8, where Fig. 8a corresponds to the results of the proposed algorithm, and Fig. 8b to the results of the adaptive threshold algorithm [15] considering $a = 3$.

In Fig. 8, the circles indicate magnified areas, and the raw scanning data is split into different segments indicated in different colors. In addition, the figure shows outliers removal when using both SEF algorithms. The black circles in Fig. 8a indicate profiles preserved by the proposed algorithm, whereas information of structures with large deflection an-

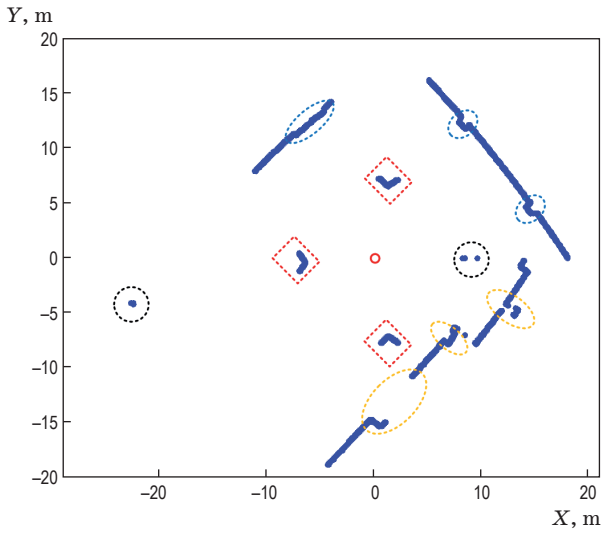

Fig. 7. Raw measured points in a parking lot.

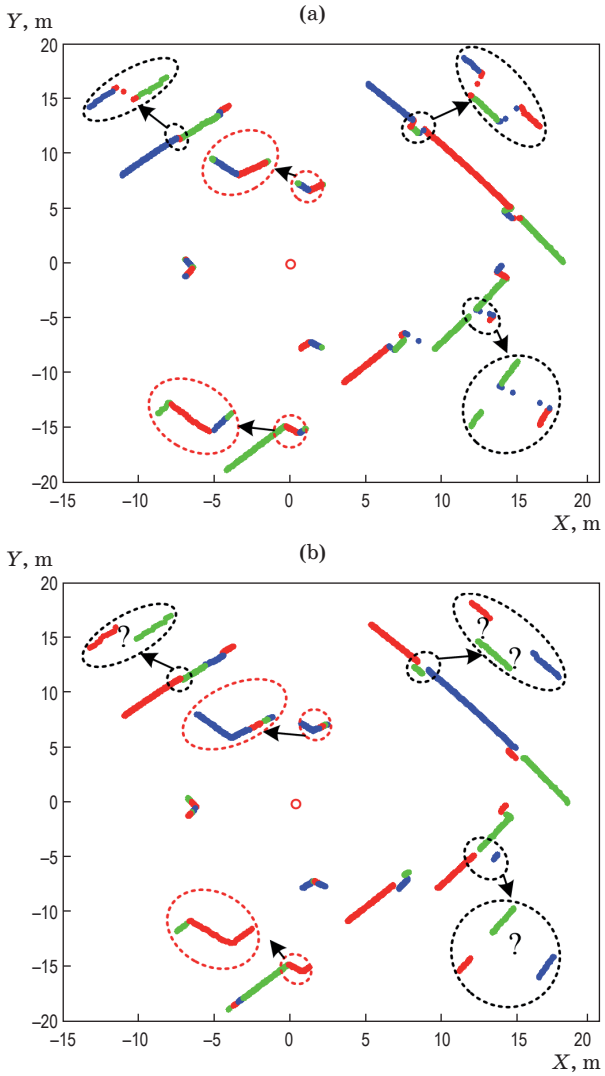

Fig. 8. Segmentation result after applying the proposed algorithm based on local oscillation (a) and the adaptive threshold algorithm (b).

gles has been removed by the comparison algorithm in Fig. 8b. Furthermore, the red circles indicate the separation of corner segments achieved by the proposed algorithm but not by the adaptive threshold algorithm, which requires further processing to identify corners.

Then, we applied the merge step to prevent overfitting during segmentation, whose results, which are shown in Fig. 9, demonstrate that fragments corresponding to the same line segment have been merged into one cluster when compared to Fig. 8. Note that the protruding and embedded structures have been preserved. After merging, we obtained 34 line segments representing the parking lot.

The parameters of the 34 line segments were determined after merging, and the corners were clearly

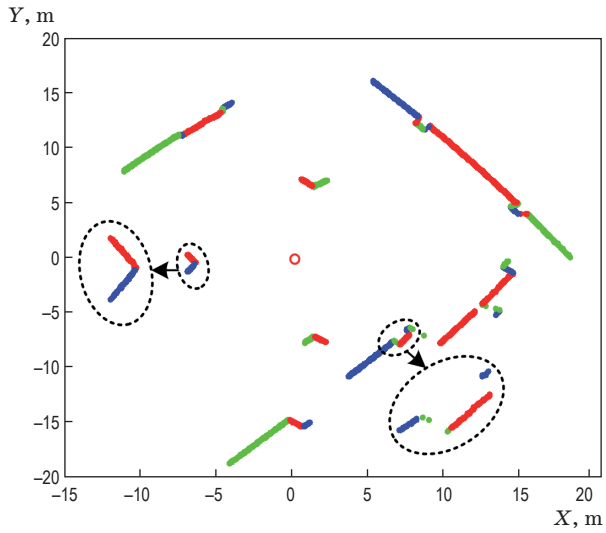

Fig. 9. Results of the proposed algorithm after merging with $D_T = 30$ cm, $\gamma_T = 30°$.

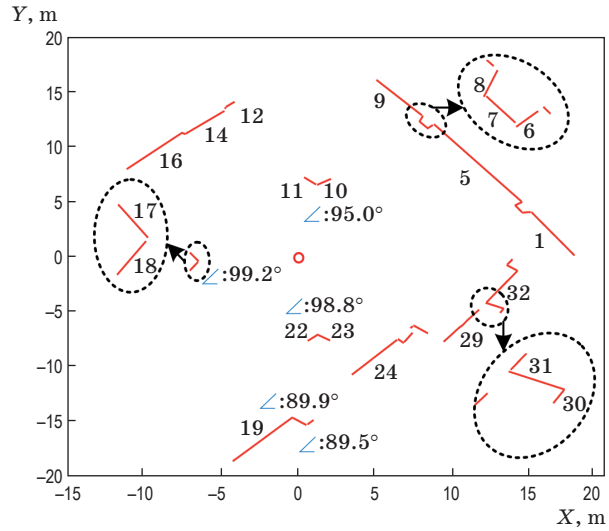

Fig. 10. Environment reconstruction represented by line segments and corners.

determined without requiring further processing, as shown in Fig. 10. The line segments of the surfaces are indicated with numbers. The corner angles were accurately determined, and slopes with large deflection with respect to the laser sensor in the protruding and embedded structures were completely preserved (e.g., line segments 6, 8, and 31). Information preservation is an important feature for mobile robots to successfully perceive their surroundings.

5. CONCLUSIONS

We derive a more realistic 2D laser detection model and propose an improved SEF algorithm based on local deflection to prevent the information loss that usually occurs in conventional SEF algorithms. In addition, we include three constraints to further improve robustness and efficiency of the algorithm. Likewise, a merge step prevents overfitting during segmentation, and the LSM is used to estimate the line parameters and identify corners. The 2D reconstruction of an underground parking lot verifies the accuracy and efficiency of the proposed algorithm. In future developments, we will include the line scanning information estimated by the laser sensor to extend the algorithm for three-dimensional real-time simultaneous localization and mapping for mobile robots aiming to improve accuracy.

DISCLOSURES

The authors have no conflicts of interest to declare.

REFERENCES

1. *He X., Cai Z.* Feature extraction from 2D laser range data for indoor navigation of aerial robot // IEEE CAC. 2013. P. 306–309.
2. *Yin J., Carlone L., Rosa S., Bona B.* Graph-based robust localization and mapping for autonomous mobile robotic navigation // IEEE ICMA. 2014. P. 1680–1685.
3. *An S.-Y., Kang J.-G., Lee L.-K., Oh S.-Y.* SLAM with salient line feature extraction in indoor environments // IEEE ICARCV. 2011. P. 410–416.
4. *Nguyen V., Martinelli A., Tomatis N., Siegwart R.* A comparison of line extraction algorithms using 2D laser rangefinder for indoor mobile robotics // IEEE/RSJ IROS. 2015. P. 1929–1934.
5. *Nguyen V., Gächter S., Martinelli A., Tomatis N., Siegwart R.* A comparison of line extraction algorithms using 2D range data for indoor mobile robotics // IEEE/RSJ IROS. 2005. P. 97–111.
6. *Premebida C., Nunes U.* Segmentation and geometric primitives extraction from 2D laser range data for mobile robot applications // Robotica. 2005. P. 17–25.
7. *Rasheed U., Ahmed M., Ali S., Afridi J., Kunwar F.* Generic vision based algorithm for driving space detection in diverse indoor and outdoor environments // IEEE ICMA. 2010. P. 1609–1614.
8. *Victorino A.C., Rives P.* Bayesian segmentation of laser range scan for indoor navigation // IEEE/RSJ IROS. 2004. P. 2731–2736.
9. *Siadat A., Kaske A., Klausmann S., Dufaut M., Husson R.* An optimized segmentation method for a 2D laser-scanner applied to mobile robot navigation // Proceedings of the 3rd IFAC Symposium on Intelligent Components and Instruments for Control Applications. 2007. P. 153–158.
10. *Borges G.A., Aldon M.J.* Line extraction in 2D range images for mobile robotics // Journal of Intelligent and Robotic Systems. 2004. P. 267–297.
11. *Duda R.O., Hart P.E.* Pattern classification and scene analysis. New York: John Wiley, 1973. P. 183–196.
12. *Pavlidis T., Horowitz S.L.* Segmentation of plane curves // IEEE Transactions on Computers. 1974. P. 860–870.
13. *Bolles R.C., Fischler M.A.* A RANSAC-based approach to model fitting and its application to finding cylinders in range data // Proceedings of the 7th International Joint Conference on Artificial Intelligence. 1981. P. 637–643.
14. *Duda R.O., Hart P.E.* Use of the Hough transformation to detect lines and curves in pictures // Communications of the ACM. 1972. P. 11–15.
15. *Bu Y., Zhang H., Wang H., Liu R., Wang K.* Two-dimensional laser feature extraction based on improved successive edge following // Appl. Opt. 2015. P. 4273–4279.